J Membrane Biol (2014) 247:469–477
DOI 10.1007/s00232-014-9653-0

Supercritical CO_2 Induces Marked Changes in Membrane Phospholipids Composition in *Escherichia coli* K12

Sabrina Tamburini · Andrea Anesi · Giovanna Ferrentino · Sara Spilimbergo · Graziano Guella · Olivier Jousson

Received: 30 October 2013 / Accepted: 7 March 2014 / Published online: 22 March 2014

Abstract Supercritical carbon dioxide (SC-CO_2) treatment is one of the most promising alternative techniques for pasteurization of both liquid and solid food products. The inhibitory effect of SC-CO_2 on bacterial growth has been investigated in different species, but the precise mechanism of action remains unknown. Membrane permeabilization has been proposed to be the first event in SC-CO_2-mediated inactivation. Flow cytometry, high performance liquid chromatography–electrospray ionization–mass spectrometry and NMR analyses were performed to investigate the effect of SC-CO_2 treatment on membrane lipid profile and membrane permeability in *Escherichia coli* K12. After 15 min of SC-CO_2 treatment at 120 bar and 35 °C, the majority of bacterial cells dissipated their membrane potential (95 %) and lost membrane integrity, as 81 % become partially permeabilized and 18 % fully permeabilized. Membrane permeabilization was associated with a 20 % decrease in bacterial biovolume and to a strong (>50 %) reduction in phosphatidylglycerol (PG) membrane lipids, without altering the fatty acid composition and the degree of unsaturation of acyl chains. PGs are thought to play an important role in membrane stability, by reducing motion of phosphatidylethanolamine (PE) along the membrane bilayer, therefore promoting the formation of inter-lipid hydrogen bonds. In addition, the decrease in intracellular pH induced by SC-CO_2 likely alters the chemical properties of phospholipids and the PE/PG ratio. Biophysical effects of SC-CO_2 thus cause a strong perturbation of membrane architecture in *E. coli*, and such alterations are likely associated with its strong inactivation effect.

Keywords Supercritical CO_2 · *Escherichia coli* · Phosphatidylglycerol · Phosphatidylethanolamine · Membrane permeabilization

Introduction

In the last two decades, the increasing demand for both fresh ready-to-eat and off-season food products promoted the development and application of new "minimal processing" technologies for pasteurization of fresh food products. Technologies alternative to heat-based methods present the main advantage to reduce the alteration of organoleptic properties of food (Devlieghere et al. 2004). Supercritical carbon dioxide (SC-CO_2) treatment is one of the most promising alternative techniques for pasteurization of both liquid and solid food products (Ferrentino and Spilimbergo 2011; Spilimbergo and Bertucco 2003). CO_2 has bacteriostatic properties and is relatively inert, inexpensive, non-toxic, nonflammable, recyclable, readily available at high purity grades and leaves no residues (Clifford and Williams 2000). CO_2 in its supercritical state (i.e., above 73.8 bar and 31.1 °C) was demonstrated to be more efficient to inactivate

Electronic supplementary material The online version of this article (doi:10.1007/s00232-014-9653-0) contains supplementary material, which is available to authorized users.

S. Tamburini (✉) · O. Jousson
Centre for Integrative Biology (CIBIO), University of Trento, Via delle Regole 101, 38123 Trento, Italy
e-mail: tamburini@science.unitn.it

A. Anesi · G. Guella
Bioorganic Chemistry Lab, Physics Department, University of Trento, Trento, Italy

G. Ferrentino · S. Spilimbergo
Department of Materials Engineering and Industrial Technologies, University of Trento, Trento, Italy

bacteria than in its subcritical state (Garcia-Gonzalez et al. 2007). The inhibitory effect of SC-CO_2 on bacterial growth has been investigated in different species (Damar and Balaban 2006; Garcia-Gonzalez et al. 2007), but the precise mechanism of action remains unknown. An hypothesis is that SC-CO_2 reacts with water forming carbonic acid whose dissociation into hydrogen ions lowers the extracellular pH of the growth medium (Spilimbergo and Bertucco 2003; Spilimbergo et al. 2010). This situation probably affects the enzymatic activity (Ballestra et al. 1996), the intracellular electrolytic balance (Lin et al. 1993), the protein stability and the structure of nucleic acids or other organic molecules (Sahena et al. 2009; Liao et al. 2011). However, most microbes, including *Escherichia coli* and *Bacillus subtilis*, are able to maintain intracellular pH homeostasis under osmotic stress (Slonczewski et al. 2009). CO_2 diffuses into cellular membrane and may accumulate in the phospholipid bilayer, as demonstrated in yeast (Isenschmid et al. 1995). The accumulation of CO_2 increases the fluidity of membrane due to a loss of order of the lipid hydrophobic chains leading to the so-called "anesthesia effect." Additional effects include destabilization of essential membrane domains and an increase in permeability (Jones and Greenfield 1982; Isenschmid et al. 1995). Permeabilization of the cell membrane has been proposed to be the first event leading to cell inactivation or death (Garcia-Gonzalez et al. 2007; Spilimbergo et al. 2009). Membrane permeabilization in *E. coli* and *L. monocytogenes* cells induced by SC-CO_2 was investigated by Garcia-Gonzalez et al. (2010) using spectrofluorometry and transmission electron microscopy. These authors demonstrated the relationship between irreversible membrane permeabilization and the inability of bacteria to grow on rich media. Membrane permeabilization induced by SC-CO_2 was also observed in *Salmonella enterica* (Kim et al. 2009; Tamburini et al. 2013) and in *Saccharomyces cerevisiae* (Spilimbergo et al. 2010) by using flow cytometry (FCM) coupled with viable dyes. However, whether SC-CO_2 has a direct effect on bacterial membrane or permeabilization is a consequence of cell death remains an open question. Kim et al. (2009) applied GC–MS to analyze fatty acid profiling of *S. enterica* serotype *Typhimurium*. Their results suggested that the inactivation of *Salmonella* could be related to an increase in minor compounds in the fatty acid profile, though SC-CO_2 could also alter the membrane so that minor fatty acids become more efficiently extracted. SC-CO_2 is indeed used as a solvent to extract non-polar compounds such as triglycerides and fats (Sahena et al. 2009).

The aim of this study was to provide new insights on the action of SC-CO_2 treatment on bacterial membranes. We performed detailed FCM analysis coupled with viability dyes to assess bacterial permeabilization and high performance liquid chromatography–electrospray ionization–mass spectrometry (LC–ESI–MS) as well as ^{31}P-NMR analyses to examine the membrane lipid profile of *E. coli* K12 under SC-CO_2 treatment. We report significant alterations in membrane composition potentially leading to membrane instability and permeabilization.

Materials and Methods

Bacterial Strains and Growth Media

Escherichia coli K12 MG1665 was grown on solid Luria–Bertani (LB) agar medium (Sigma-Aldrich Co., Milan, Italy) at 37 °C for 16 h. One colony was picked, inoculated into 10 ml of LB medium and incubated at 37 °C with constant shaking (200 rpm) to stationary phase (16 h). The cells were re-inoculated into 200 ml of LB medium and incubated at 37 °C with constant shaking (200 rpm) to reach the exponential phase, with OD = 0.6).

SC-CO_2 Treatment

SC-CO_2 treatment was performed in a multi-batch apparatus as described by Mantoan and Spilimbergo (2011). Briefly, the system consisted of 10 identical 15-ml-capacity reactors operating in parallel. All reactors were submerged in the same temperature-controlled water bath to maintain the desired temperature constant throughout the process. Each reactor was connected to an on–off valve for independent depressurization and had an internal magnetic stirrer device, to guarantee homogeneous dissolution of SC-CO_2 in the cell suspension. 10 ml of *E. coli* cells grown in LB medium, at a concentration of 4×10^8 cells/ml, were loaded into each reactor. Bacteria were treated with SC-CO_2 at 120 bar and 35 °C, at 500 rpm and up to 60 min. Two different untreated samples were used as control samples: 0_{out} control was collected at $t = 0$ and maintained at 4 °C, while 0_{in} control was placed in the reactor at 120 bar, 35 °C and 500 rpm, without exposure to SC-CO_2 and collected after 45 min. The 0_{out} control was used for 5 min and 15 min treatment time points, whereas the 0_{in} control was used for 30 min and 45 min treatment time points, because cells kept in the reactor at 35 °C for more than 20 min could replicate.

Flow Cytometry

Untreated and SC-CO_2-treated samples were diluted to 10^7–10^8 cells/ml and divided in two subsamples. One ml of each sample was stained with 10 µl SYBR-I (Merck, Darmstadt, Germany), at 1:30,000 final concentration in DSMO and 10 µl of Propidium Iodide (PI) at 1 mg/ml (Invitrogen, Carlsbad, CA, USA) to quantify intact and

permeabilized cells (Ziglio et al. 2002). The depolarized cells were measured adding 10 µl of 1 mM $DiBAC_4(3)$ (Invitrogen, Carlsbad, CA, USA), and only *E. coli* depolarized cells emit green fluorescence, and the percentage of depolarized cells was calculated using the total count measurements (Berney et al. 2006). Excitation and emission wavelengths were at $\lambda_{ex} = 495$ nm, $\lambda_{em} = 525$ nm for SYBR-I; $\lambda_{ex} = 536$ nm, $\lambda_{em} = 617$ nm for PI and $\lambda_{ex} = 490$ nm, $\lambda_{em} = 516$ nm for $DiBAC_4(3)$. Samples were incubated at room temperature, in the dark for 15 min. FCM analyses were performed with an Apogee-A40 flow cytometer (Apogee Flow Systems, Hertfordshire, UK) equipped with an Argon laser emitting at 488 nm. For each cell crossing the focus point of the laser, two light scattering signals and two fluorescence signals (green, FL1 and red, FL3) were collected. The large angle light scatter (LALS), measuring cell density or granularity (Müller and Nebe-von-Caron 2010), and the forward angle light scatter (FALS), which is related to bacterial size (Foladori et al. 2008), were measured. LALS and FALS were collected on a 256-channel linear scale, while fluorescence signals were collected with logarithmic amplifier gain. The conversion of FALS intensities into biovolumes was performed as proposed by Foladori et al. (2008). Non-fluorescent silica microspheres (MicroParticles GmbH, Germany) of different diameters were used to assess the calibration curve of FALS intensity used in bacterial sizing. Six sizes of silica microspheres with diameters ranging from 0.5 to 1 µm were selected.

Phospholipid Extraction

About 10^9 *E. coli* cells (untreated and treated) were collected by centrifugation at 6,000 rpm for 10 min. The pellets were suspended into 500 µl of sterile water. Seventy-five microliters of a 10 ng/µl methanolic solution of phosphatidylcholine (PC), PC 12:0/12:0 (Avanti Lipids In., Alabama, US), was added to each sample as internal standard for evaluating the efficiency of extractions, followed by 3 ml of $CHCl_3/CH_3OH$ (2:1) solution for phospholipid extraction (Carlo Erba, Milan, Italy). Bacterial cells were disrupted by using an Ultrasound processor S-4000 sonicator (Misonix. Inc, Farmingdale, NY, USA) operating at 20 kHz. Each sample was subjected to two cycles of sonication with the following program: treatment time of 150 s, amplitude of 40, pulse time 3 s and pause time 2 s. The main parameters (transferred power, P; time, t; treated volume, V) were used to calculate the transferred specific energy as reference parameter, indicated afterward as Es and expressed in kJ/l ($Es = Pxt/V$). Transferred power instead of applied power was used for Es calculation, in order to obtain results comparable with those obtained from different instruments. After sonication, the samples were centrifuged for 10 min at 10,000 rpm and at 4 °C. The lower organic phase of each sample was recovered, brought to dryness and re-suspended in 300 µl of methanol for liquid chromatography–mass spectrometry (LC–MS) analyses. Preliminary ^{1}H- and ^{31}P-NMR analyses of phospholipids (PL) composition were also carried out on selected lipid extracts wherein internal standard PC 12:0/12:0 was not added.

NMR Measurements

^{1}H-NMR (400.13 MHz) and ^{31}P-NMR (161.98 MHz) were recorded at 300 K on a Bruker-Avance 400 MHz NMR spectrometer in CD_3OD (99 %, Aldrich) by using a 5 mm BBI probe. The ^{1}H-NMR chemical shift scale (δ) was calibrated on the residual proton signal of CD_3OD ($\delta_H = 3.310$ ppm) whereas the ^{31}P-NMR scale (δ) on the signal of the commercially available PC 18:1/18:1 ($\delta_P = -0.55$ ppm). Since all these spectra were acquired in the same conditions and by using the same acquisition parameters, this acts as an external standard and allowed us to fix the *x*-axis of all our ^{31}P-NMR spectra. Composite pulse decoupling was used to remove any proton coupling in ^{31}P-NMR spectra. Generally, 4,000 free induction decays were processed using an exponential line broadening of 0.3 Hz prior to Fourier transformation. Probe temperature was maintained to ±0.1 °C by a Bruker B-VT 1000 variable temperature unit. Resulting 1D NMR spectra were analyzed by MestreNova 8.1 software (Mestrelab research S.L.2012, Escondido, CA).

HPLC–ESI–MS Analysis

The raw methanol extract was analyzed by LC–MS using a Hewlett-Packard Model 1100 series liquid chromatograph coupled to a Bruker Esquire-LC^{TM} quadrupole ion-trap mass spectrometer (Bruker-Franzenm Bremen, Germany) equipped with electrospray ion source (ESI). The chromatographic separation of PL was carried out at room temperature on a Kinetek^{TM}C18 column (length: 100 mm; particle size: 2.6 µm; internal diameter: 2.1 mm; pore size: 100 Å) purchased by Phenomenex (Torrence, Ca, USA). The solvent system consisted of A, CH_3OH/H_2O 7:3 containing 12 mM ammonium acetate and B, CH_3OH also containing 12 mM ammonium acetate. The linear gradient, at a constant flow rate of 1.0 ml/min, started from 30 % B to reach 100 % B in 40 min, followed by column wash using 100 %B for 15 min and column re-equilibration at starting conditions. Nebulizer gas was high purity nitrogen at a pressure of 20–30 psi, at a flow of 6 l/min and 300 °C. The mass spectrometer scan range was 13,000 units per second in the range 50–1,500 *m/z* with a mass accuracy of about 100 ppm which translates to about ±0.07 Da for a

molecule with a mass of 700 Da. The ESI was operated in positive ion mode for PC analysis and in negative ion mode for phosphatidylglycerol (PG) and phosphatidylethanolamine (PE) analysis. For the quantitation of lipid species, the extracted ion chromatograms from negative ion full scan data were integrated using DataAnalysis 3.0 software (Bruker Daltonik, Bremen, Germany). The correct assignment of *m/z* values to PE and PG species was carried out by the analysis of negative and positive ion scan data. In particular, the negative ion mode provides information about molecular ions and fatty acyl chains while positive ion mode were employed to confirm the correct assignment by analyzing the neutral loss of polar head. To strengthen our analysis, we also carried out neutral loss and precursor ion scan experiments, in positive ion mode, on selected samples by using a Triple Quadrupole mass spectrometer. For each replicate, we calculated the % molar ratio PE/PG by summing total area of PE and PG species, corrected by the response factor. A mixture consisting of equimolar amount of the commercially available lipids PC 17:0/20:4, PE 17:0/20:4 and PG 17:0/20:4 (Avanti Polar Lipids, Inc. Alabama, USA) was used to prepare a suitable working curve to use as an external tool to normalize the different ESI response factors of PC, PE and PG in our ESI–MS instrumental setup. The MS-data of every PL species in each sample were finally normalized to the recovery value and to the number of starting cells. The relative abundances of all the lipids species here reported were established by assuming the same response factor for all the lipid species belonging to a given lipid class (PE or PG); since this assumption is somehow arbitrary, this relative distribution is better expressed as the % area ratio of the intra-class lipids rather than their molar fraction. In fact, as there are differences in the ionization process of various PLs depending on their acyl chains length, number of unsaturations and relative concentrations, the individual mass spectra may not accurately reflect the molar composition of each sample. However, since we are essentially interested to relative variation in lipid composition between untreated and SC-CO_2-treated cells, the % peak area ratio is an adequate observable.

Results

SC-CO_2– Induced Depolarization, Permeabilization and Biovolume Reduction in *E. coli*

As previously reported (Tamburini et al. 2013), the double staining with SYBR-I and PI in FCM analysis allowed to distinguish different bacterial subpopulations: (1) intact cells, emitting green fluorescence; (2) partially permeabilized cells, emitting both green and red fluorescence and (3) permeabilized cells, emitting red fluorescence. Figure 1 shows the distribution of *E. coli* subpopulations as a function of treatment times. After 15 min of SC-CO_2 treatment, a significant effect on the membrane was observed, as 18 % of cells were permeabilized and 81 % were partially permeabilized. Cell depolarization also became effective after 15 min. For longer treatment times, the partially permeabilized cells became permeabilized and the proportion of depolarized cells decreased. These results indicate that partial permeabilization leads to depolarization of the membrane. When the cells become fully permeabilized, $DIBAC_4(3)$ dye likely diffuses out of the cells. The comparison between untreated and SC-CO_2-treated samples did not show significant differences of LALS signals, indicating that the treatment has no detectable effect on cell density or granularity (data not shown). Conversely, FALS signals, which provide information on cellular biovolume, changed significantly after 15 min of treatment (Fig. 2a). Referring to an arbitrary scale divided in 256 channels, the FALS peak of untreated and treated cells was at 126 and 98 mean channel, respectively. The biovolume ratio was 1.3, indicating that the cellular biovolume decreased of about 20 % after 15 min; longer treatment times did not induce further biovolume reduction (Fig. 2b).

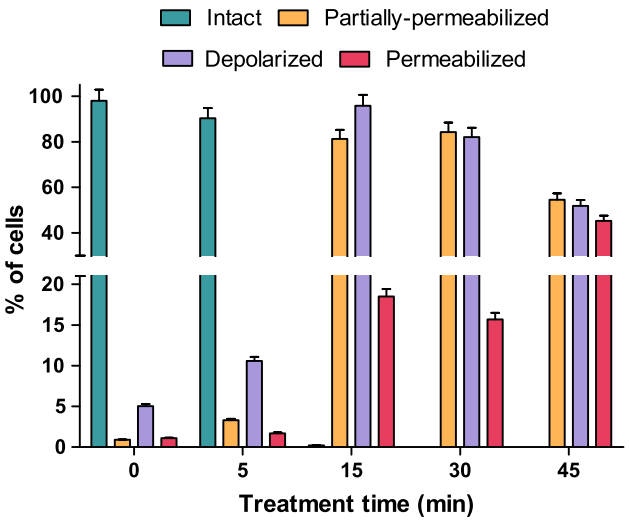

Fig. 1 Proportions of intact, partially permeabilized, permeabilized and depolarized *E. coli* cells during SC-CO_2 treatment assessed by FCM

Changes in Cell Membranes Lipid Composition by NMR

A preliminary NMR analysis was carried out in order to establish the phospholipid profile of *E. coli* membranes. The ^{1}H-NMR spectrum of a raw lipids extract (Fig. 3a)

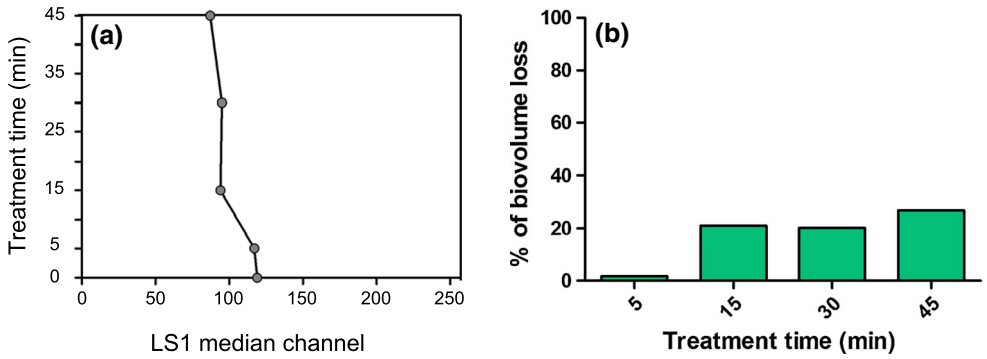

Fig. 2 Reduction in cellular biovolume and PL during SC-CO_2 treatment. **a** Median channels of FALS signals and **b** associated percentages of biovolume reduction

clearly indicated the dominance of PE lipids species by the characteristic resonances of the ethanolamine head group (δ_H 3.16 and 4.03 for the methylene protons linked to α-carbon atoms at amino- and phosphate group, respectively) besides the expected proton-resonances attributable to the presence of two acyl chains on the glycerol backbone (multiplets at δ_H 5.23 and 4.44/4.18 for protons linked carbon atoms at *sn*-1 and *sn*-2 position of glycerol, respectively) and the presence of unsaturation on the same chains (triplet at δ_H 5.35). A characteristic multiplet at δ_H 3.76 attributable, by comparison with ^{1}H-NMR spectra of commercially available PG 16:0/18:0, to proton linked at *sn*-2 position of the free glycerol moiety of PG lipid species was also detected. Finally, the evaluated PG/PE molar ratio (16 %, defined by the ratio of the normalized NMR area of PG with respect to that of PE), must be considered just a rough estimation due both to the low signal/noise ratio of the spectrum and partial overlap of the PE/PG signals considered in the corresponding area integrations. Further structural information was gained by ^{31}P-NMR measurements (Fig. 3b) carried out in CD_3OD. The perfect correspondence of the two ^{31}P resonances detected in *E. coli* extracted samples at δ_P 0.18 and 0.73 ppm with those of solutions of the commercially available PE (δ_P 0.18) and PG (δ_P 0.73) allowed us to firmly establish the presence of these two main PL classes in *E. coli* samples. Moreover, the area integrations of these two ^{31}P-NMR signals allowed us to reliably establish their % molar fractions obtaining $x_{PE} = (82 \pm 2)$ % and $x_{PG} = (18 \pm 2)$ %.

The same analysis carried out on a sample obtained by extraction of SC-CO_2-treated cells (60 min) gave us the first suggestion that the PG/PE ratio undergoes strong control by SC-CO_2 treatment. In fact, after overnight acquisition of the corresponding ^{31}P-NMR spectrum, the signal of PG was found significantly decreased with respect to that of PE as much to hinder a reliable integration of the PG signal itself.

Optimization of HPLC/ESI–MS System

In our optimized LC system, based on reversed-phase stationary phase and on a gradient of methanol/water (containing the ion-pairing ammonium acetate) solution as mobile phase, lipid species were efficiently separated on the basis of the elution time. Each PG species had a lower retention time (t_R) compared to the corresponding PE species (e.g., PG 34:1 and PE 34:1 have t_R 15.3 min and 22.1 min, respectively). Within a given PL species, each increase in $–CH_2–CH_2–$units within acyl chains increases the t_R of about 5 min, while t_R decreases of more than 3 min for the increase in every single unsaturation. Thus, phospholipid species with less unsaturated and/or longer acyl chain lengths eluted at higher t_R than saturated and/or shorter ones. As a consequence, the LC chromatogram showed a partial overlap of longer and/or less unsaturated PG species with shorter and/or more unsaturated PE species. However, this outcome did not hinder the MS analysis since the ESI(−) spectra of these eventually overlapped PG and PE species were clearly different and promptly attributed.

Phospholipid Profiles of *E. coli* by LC–MS

Full scan ESI(−)-MS spectra were a powerful tool to attribute each peak in the MS-chromatogram to a distinct PL species. In particular, all the PG and PE species showed both the strong parent ion $[M–H]^-$ and some characteristic daughter ions deriving from in-source collision-induced dissociation of the parent ion itself. Among them, the carboxylates R_1COO^- and R_2COO^- anions were quite important to establish the structural formula of every species belonging to these two PL classes. As an example, a chromatographic peak at 21.1 min showed its parent ion $[M–H]^-$ at *m/z* 716 and daughter ions at *m/z* 281 (18:1) and 255 (16:0) was promptly attributed to PE 18:1/16:0 (=PE

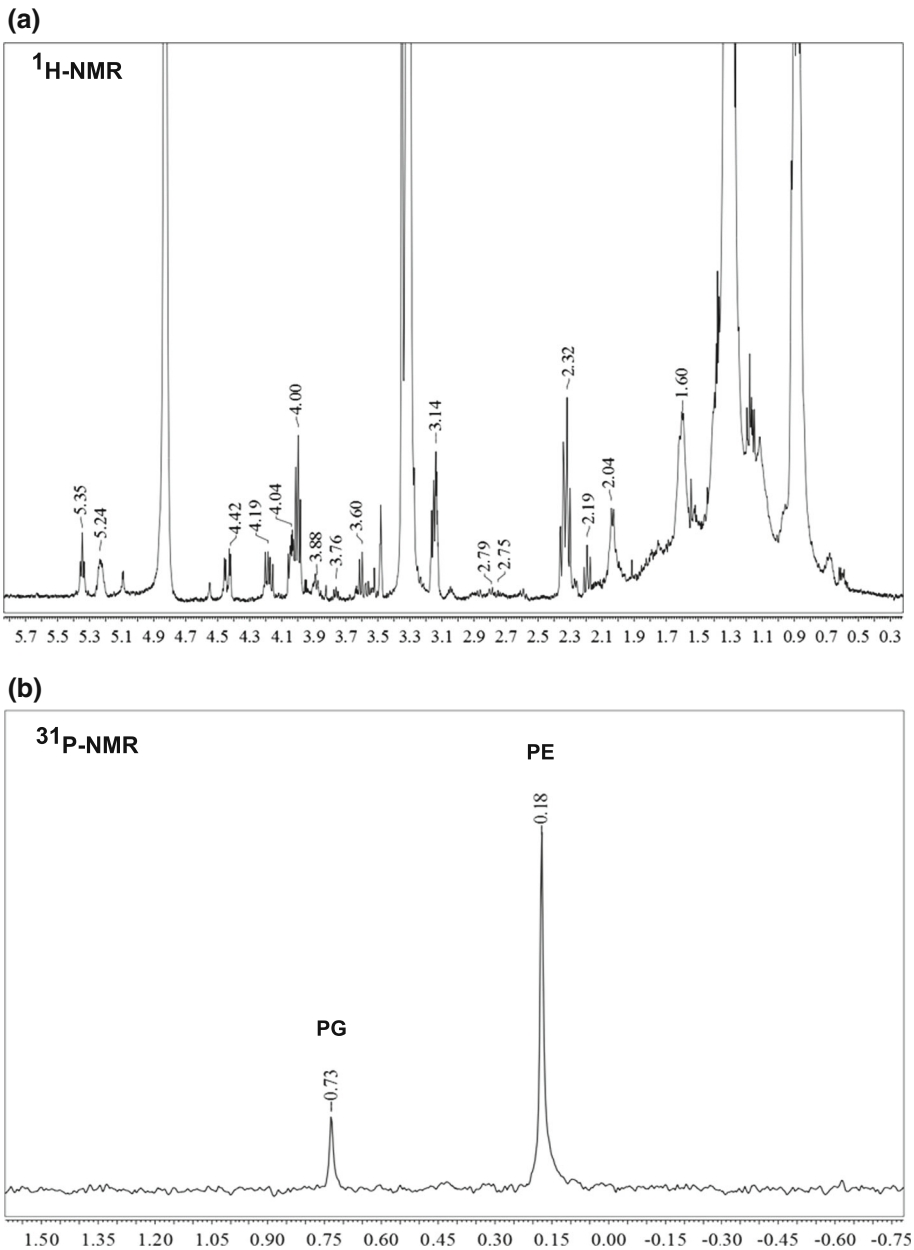

Fig. 3 NMR spectra acquired at 300 K in CD_3OD on a raw extract, of phospholipid profile in *E. coli* K12 cells. **a** ^{1}H-NMR (400 MHz) spectrum **b** ^{31}P-NMR (161 MHz) spectrum

34:1), whereas a chromatographic peak at 11.4 min showed its parent ion $[M–H]^-$ at *m/z* 745 and daughter ions at at *m/z* 281 (18:1) and 253 (16:1) was promptly attributed to PG 18:1/16:1 (=PG 34:2).

With the insight gained by preliminary NMR measurements *E. coli* lipid profile was performed by mass spectrometric techniques, in particular through HPLC/ESI–MS. A complete qualitative analysis carried out on *E. coli* cells confirmed the previous NMR findings, which showed that more than 98 % of our sample contained only PE and PG lipids. However, a wide chemical diversity of the acyl chains was found both in PE (25 species) and PG (22 species) with principally saturated and mono-unsaturated chains whose length ranged from 14 to 19 carbon atoms. A relevant source of chemical diversity was found to derive from the presence in significant amount of (1) odd carbon atoms acyl chains (in particular 15:0 and 17:1) and (2) structural and regiochemical isomers (such as PE 16:0/18:1 and PE 18:1/16:0). The complete lipid profile of the *E. coli* cells is reported in Fig. 4 and in the Table 1 of Supplementary Material. Among all PL species, PE 32:1, 34:1, 34:2 and 36:2 were found to dominate but even PE 30:0, 30:1, 32:1, 32:2 and 33:1 were present in relative amount higher than 2 %; PG species were found in much lower amount than PE, but essentially they shared the same acyl chains of PE species. According to Morein et al. (1996) and

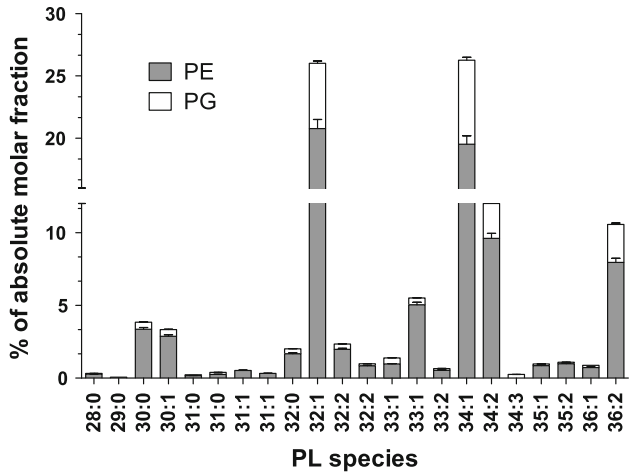

Fig. 4 Phospholipid profile of *E. coli* K12 MG1665. The percentage of absolute molar fraction of each PE or PG species are indicated

Lu et al. (2011) and our ^{31}P-NMR measurements, the average molar fraction of all the PEs in *E. coli* cells was evaluated to be $x_{PE} = (80 \pm 3)$ %, while $x_{PG} = (20 \pm 2)$ %.

SC-CO_2 Effect on PGs, and PEs and Acyl Chains

Full quantitative analyses were performed through HPLC/ESI–MS to compare *E. coli* lipids profile between untreated and SC-CO_2-treated samples. The *E. coli* cells were treated at 120 bar, 35 °C up to 30 min. The integration of the extracted ion currents of all the PL species allowed to establish, through external calibration (working curve) and normalization of the recovery efficiency of every extraction (by addition of a known amount of PC 12:0/12:0), the complete quantitative profile of the samples. The comparison of PE (Fig. 5a) and PG (Fig. 5b) quantitative profile of untreated and treated samples not only confirmed the first NMR results, but also allowed to gain much more structural details. First of all, the PG/PE molar ratio was found to be much lower in treated samples. The absolute amount of total PL showed only marginal change although the absolute amount of the PG species underwent a strong reduction (52 % after 30 min, Fig. 5b); the PG decrease resulted somehow compensated by small increase in the amount of the PE species. In particular, the percentage absolute molar fraction (%amf) of PE species, defined as %amf (PE) = $[\Sigma_i \text{mol(PE)}_i/\text{total mol (PL)}] \times 100$, changed from 80 % (untreated) to 90 % (after 30 min of treatment), while the corresponding %amf of PG species [%amf (PG) = $[\Sigma_i \text{mol(PG)}_i/\text{total mol(PL)}] \times 100$)] changed from 20 % (untreated) to 10 % (after 30 min of treatment) with respect to total PL; a significant part of PG reduction was obtained in the first 5 min of treatment where the PG

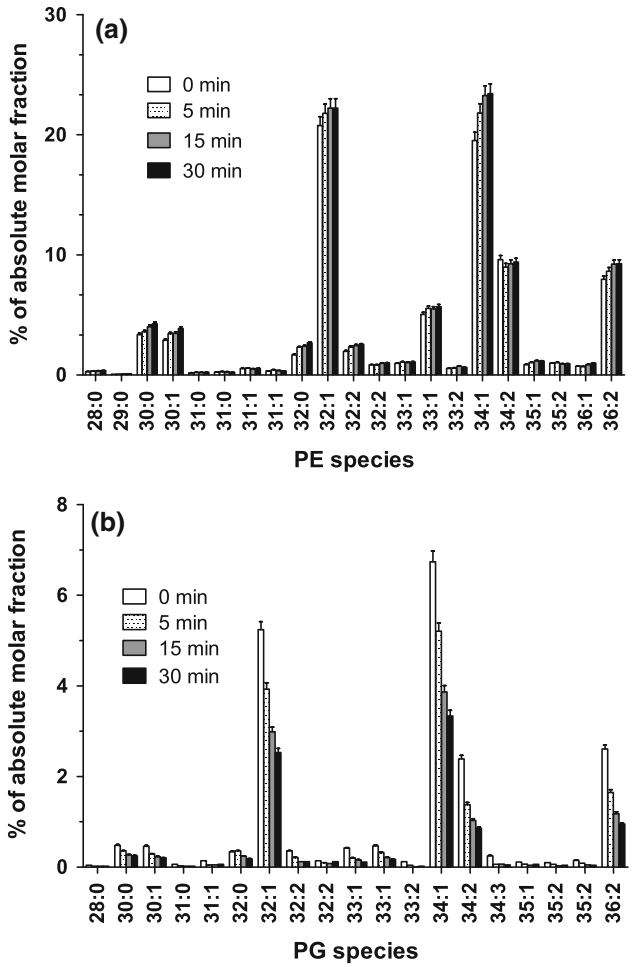

Fig. 5 Quantitative lipids profile of untreated and SC-CO_2-treated *E. coli* cells: **a** PE species and **b** PG species

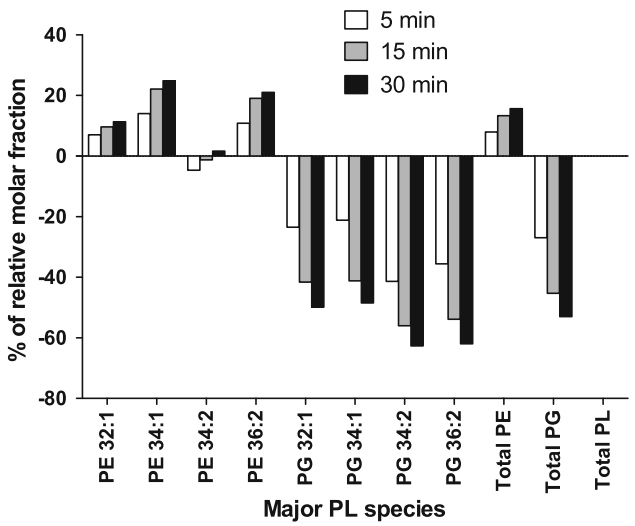

Fig. 6 Percentages of relative molar fraction of the major PL species detected in *E. coli* K12 after SC-CO_2 treatment

species were reduced of 30 % with respect to the amount of PGs in untreated samples (60 % of the overall observed reduction) (Fig. 6).

The % relative molar fraction (%rmf) of single species belonging to a given PL class (for PE class defined as %rmf (PE) = $[\Sigma_i mol(PE)_i/total\ mol\ (PE)] \times 100$ and for PG class as %rmf (PG) = $[\Sigma_i mol(PG)_i/total\ mol\ (PG)] \times 100$) did not show statistically significant changes in % rmf (PE) and % rmf (PG) after treatment, indicating that SC-CO_2 acted with the same effects on all PE or PG species. The HPLC/ESI–MS permitted to determine whether SC-CO_2 treatment induced changes in the unsaturation index (UI) and in the length of lipid chains (LLC). UI was here defined as $UI = \Sigma_i\ (UN)_i \times (amf)_i$, where UN represent the number of double bonds and amf the absolute molar fraction of a given species *i,* and the sum is extended on all the PE and PG species. The data clearly indicated that UI (1.16 ± 0.02) did not show any change during the treatment. The same behavior was followed also by LLC (defined by $\Sigma_i\ (LLC)_i \times (amf)_i$,) which was found (33.10 ± 0.03) absolutely constant during the time course of the treatment.

Discussion

In this study, the changes of lipid profiles in *E. coli* K12 induced by SC-CO_2 treatment were compared with cellular features to get insights on the action mechanism of SC-CO_2 on bacterial cells. After 15 min of SC-CO_2 treatment, most of bacterial cells lost their membrane potential (95 %) and membrane integrity (81 % of permeabilized and 18 % of partially permeabilized cells). Bacterial permeabilization was associated with a 20 % decrease in cellular biovolume and to a strong decrease (>50 %) of PG membrane lipids.

PEs are zwitterionic lipids participating in a multitude of cellular tasks, such as cellular fusion and vesiculation, curvature bilayers, influencing permeation through the membrane and cell division (Zhao et al. 2008). Conversely, PGs are anionic carrying a unit negative charge, playing an important role in the overall homeostatic equilibrium of cell membranes and in membrane-peptide interactions (Tari et al. 1989). Due to ammonium group in PE and hydroxyl groups in PG, both lipids are able to form hydrogen bonds. PE–PE hydrogen bonds have been observed both experimentally (Boggs 1987) and in molecular simulations (Pink et al. 1998; Leekumjorn et al. 2006), whereas there is no experimental evidence of PG–PG hydrogen bonds. Zhao et al. (2008) suggested that PGs increase the bacterial membrane stability, because PGs reduce the PEs motion along bilayer, therefore promoting the formation of inter-lipid hydrogen bonds. Bacteria are able to adjust the relative concentrations of PEs and PGs when exposed to toxic organic solvents such ethanol increasing the PG/PE molar ratio (Weber et al. 1996). The lipid profiles of *E. coli*-treated cells showed that (1) SC-CO_2 treatment strongly decreased the amount of total PGs while PEs remained almost unchanged, (2) this decrease is almost uniformly distributed among all PG species and (3) the destabilizing effect induced by the PG decrease is most significant in the first minutes of the treatment.

Besides changing the headgroup of the PL species, bacteria generally respond to environmental stress by increasing the number of unsaturated fatty acids and the length of acyl chains (Weber and de Bont 1996 Zhang and Rock 2008). The data showed that both the factors did not play any role during SC-CO_2 treatment; in fact, neither the average UI (1.16 ± 0.02) nor the average acyl chain on the glycerol backbone (33.10 ± 0.03) were affected.

The intracellular pH in *Listeria monocytogenes* cells treated with SC-CO_2 was shown to decrease even below pH 5 (Spilimbergo et al. 2010). The pH change likely has detrimental effects on several biochemical processes, leading to protein denaturation, loss of enzymatic activity and changes in the structural architecture of cells membranes. Also the PE/PG ratio in cell membranes would be strongly affected by pH change, given that at pH 7 PGs are negatively charged and PEs are zwitterionic, while at pH 2.8, the phosphodiester group of PGs (pKa = 2.9) is mainly protonated (60 %) (Garidel et al. 1997). This biophysical effect could explain why SC-CO_2 treatment results in a strong perturbation of membranes architecture in *E. coli*, where PG and in particular PE have been ever found as the dominant phospholipid species. Such alterations are likely associated with its strong inactivation effect. Why specifically PG species have been found to strongly decrease during treatment requires further investigations. Future studies, including phospholipid biosynthesis mutant analysis, will help to better understand the SC-CO_2 mechanism of action and bacterial response to the treatment.

References

Ballestra P, Abreu Da Silva A, Cuq JL (1996) Inactivation of *Escherichia coli* by carbon dioxide under pressure. J Food Sci 61:829–836

Berney M, Weilenmann HU, Egli T (2006) Flow-cytometric study of vital cellular functions in *Escherichia coli* during solar disinfection (SODIS). Microbiol 152:1719–1729

Boggs JM (1987) Lipid intermolecular hydrogen bonding: influence on structural organization and membrane function. Biochim Biophys Acta 906:353–404

Clifford AA, Williams JR (2000) Introduction to supercritical fluids and their applications. In: Williams JR, Clifford AA (eds) In supercritical fluid methods and protocols. Human Press Inc., Totowa, NJ, pp 1–16

Damar S, Balaban O (2006) Review of dense phase CO_2 technology: microbial and enzyme inactivation, and effects on food quality. J Food Sci 71(1):R1–R11

Devlieghere F, Vermeiren L, Debevere J (2004) New preservation technologies: possibilities and limitations. Int Dairy J 14:273–285

Ferrentino G, Spilimbergo S (2011) High pressure carbon dioxide pasteurization of solid foods: current knowledge and future outlooks. Trends Food Sci Technol 22:427–441

Foladori A, Quaranta A, Ziglio G (2008) Use of silica microspheres having refractive index similar to bacteria for conversion of flow cytometric forward light scatter into biovolume. Water Res 42:3757–3766

Garcia-Gonzalez L, Geeraerd AH, Spilimbergo S, Elst K, Van Ginneken L, Debevere J, Van Impe JF, Devlieghere F (2007) High pressure carbon dioxide inactivation of microorganisms in foods: the past, the present and the future. Int J Food Microbiol 117:1–28

Garcia-Gonzalez L, Geeraerd AH, Mast J, Briers Y, Elst K, Van Ginneken L, Van Impe JF, Devlieghere F (2010) Membrane permeabilization and cellular death of *Escherichia coli*, *Listeria monocytogenes* and *Saccharomyces cerevisiae* as induced by high pressure carbon dioxide treatment. Food Microbiol 27:541–549

Garidel P, Christof C, Mennicke L, Blume A (1997) The mixing behavior of pseudobinary phosphatidylcholine-phosphatidylglycerol mixtures as a function of pH and chain length. Eur Biophys J 26:447–459

Isenschmid A, Marison IW, von Stockar U (1995) The influence of pressure and temperature of compressed CO_2 on the survival of yeast cells. J Biotechnol 39:229–237

Jones RP, Greenfield PF (1982) Effect of carbon dioxide on yeast growth and fermentation. Enzyme Microb Technol 4:210–223

Kim SR, Kim HT, Park HJ, Kim S, Choi HJ, Hwang GS, Yi JH, Ryu DH, Kim KH (2009) Fatty acid profiling and proteomic analysis of *Salmonella enterica* serotype *Typhimurium* inactivated with supercritical carbon dioxide. Int J Food Microbiol 134:190–195

Leekumjorn S, Sum AK (2006) Molecular investigation of the interactions of trehalose with lipid bilayers of DPPC, DPPE and their mixture. Mol Simul 32:219–230

Liao H, Zhang F, Hu X, Liao X (2011) Effects of high-pressure carbon dioxide on proteins and DNA in *Escherichia coli*. Microbiology 157:709–720

Lin HM, Yang ZY, Chen LF (1993) Inactivation of *Leuconostoc dextranicum* with carbon dioxide under pressure. Chem Eng J 52:B29–B34

Lu YH, Guan Z, Zhao J, Raetz CRH (2011) Three Phosphatidylglycerol-phosphate phosphatases in the inner membrane of *Escherichia coli*. J Biol Chem 286:5506–5518

Mantoan D, Spilimbergo S (2011) Mathematical modeling of yeast inactivation of freshly squeezed apple juice under high-pressure carbon dioxide. Crit Rev Food Sci Nut 51:91–97

Morein S, Andersson AS, Rilfors L, Lindblom G (1996) Wild-type *Escherichia coli* cells regulate the membrane lipid composition in a "window" between gel and non-lamellar structures. J Biol Chem 271(12):6801–6809

Müller S, Nebe-von-Caron G (2010) Functional single-cell analyses: flow cytometry and cell sorting of microbial populations and communities. FEMS Microbiol Rev 34(4):554–587

Pink DA, McNeil S, Quinn B, Zuckermann MJ (1998) A model of hydrogen bond formation in phosphatidylethanolamine bilayers. Biochim Biophys Acta 1368:289–305

Sahena F, Zaidul ISM, Jinap S, Karim AA, Abbas KA, Norulaini NAN, Omar AKM (2009) Application of supercritical CO_2 in lipid extraction—a review. J Food Eng 95:240–253

Slonczewski JL, Fujisawa M, Dopson M, Krulwich TA (2009) Cytoplasmic pH measurement and homeostasis in bacteria and archaea. Adv Microb Physiol 55:1–79

Spilimbergo S, Bertucco A (2003) Non-thermal bacteria inactivation with dense CO_2. Biotech Bioeng 84(6):627–638

Spilimbergo S, Mantoan D, Quaranta A, Della Mea G (2009) Real-time monitoring of cell membrane modification during supercritical CO_2 pasteurization. J Supercrit Fluids 48:93–97

Spilimbergo S, Quaranta A, Garcia-Gonzalez L, Contrini C, Cinquemani C, Van Ginneken L (2010) Intracellular pH measurement during high-pressure CO_2 pasteurization evaluated by cell fluorescent staining. J Supercrit Fluids 53:185–191

Tamburini S, Ballarini A, Ferrentino G, Moro A, Foladori P, Spilimbergo S, Jousson O (2013) Comparison of quantitative PCR and flow cytometry as cellular viability methods to study bacterial membrane permeabilization following supercritical CO_2 treatment. Microbiol 159:1056–1066

Tari A, Huang L (1989) Structure and function relationship of phosphatidylglycerol in the of phosphatidylethanolamine bilayer. Biochem 28:7708–7712

Weber FJ, de Bont JAM (1996) Adaptation mechanisms of microorganisms to the toxic effects of organic solvents on membranes. Biochim Biophys Acta 1286:225–245

Zhang YM, Rock CO (2008) Membrane lipid homeostasis in bacteria. Nat Rev 6:222–233

Zhao W, Ròg T, Andrey A, Gurtovenko AA, Vattulainen I, Karttunen M (2008) Role of phosphatidylglycerols in the stability of bacterial membranes. Biochimica 90:930–938

Ziglio G, Andreottola G, Barbesti S, Boschetti G, Bruni L, Foladori P, Villa R (2002) Assessment of activated sludge viability with flow cytometry. Water Res 36:460–468